

Zhongde SHAN, Zhi GUO, Dong DU, Feng LIU, Wenjiang LI

Digital high-efficiency print forming method and device for multi-material casting molds

© Higher Education Press 2020

Abstract Sand mold 3D printing technology based on the principle of droplet ejection has undergone rapid development in recent years and has elicited increasing attention from engineers and technicians. However, current sand mold 3D printing technology exhibits several problems, such as single-material printing molds, low manufacturing efficiency, and necessary post-process drying and heating for the manufacture of sand molds. This study proposes a novel high-efficiency print forming method and device for multi-material casting molds. The proposed method is specifically related to the integrated forming of two-way coating and printing and the short-flow manufacture of roller compaction and layered heating. These processes can realize the high-efficiency print forming of high-performance sand molds. Experimental results demonstrate that the efficiency of sand mold fabrication can be increased by 200% using the proposed two-way coating and printing method. The integrated forming method for layered heating and roller compaction presented in this study effectively shortens the manufacturing process for 3D-printed sand molds, increases sand mold strength by 63.8%, and reduces resin usage by approximately 30%. The manufacture of multi-material casting molds is demonstrated on typical wheeled cast-iron parts. This research provides theoretical guidance for the engineering application of sand mold 3D printing.

Keywords multi-material casting mold, 3D printing, efficient print forming method

Received May 24, 2019; accepted September 25, 2019

Zhongde SHAN (✉), Zhi GUO, Feng LIU, Wenjiang LI
State Key Laboratory of Advanced Forming Technology and Equipment, China Academy of Machinery Science and Technology, Beijing 100044, China
E-mail: shanzd@cam.com.cn

Zhi GUO, Dong DU
Department of Mechanical Engineering, Tsinghua University, Beijing 100084, China

1 Introduction

The foundry industry is the foundation of the manufacturing industry, and it plays an important role in many manufacturing fields, including agricultural machinery, machine tools, automobiles, ships, aerospace, defense, and military. The sand mold casting process is widely used in the foundry industry because of its advantages of abundant raw material sources, simple production processes, and numerous alloy types. The design and manufacture of casting molds and core boxes is a complicated process in the traditional sand mold casting process [1], which is characterized by long cycle length, high cost, large amount of waste materials, and low precision. These shortcomings are highlighted in the manufacture of single- and small-batch products. Sand mold 3D printing technology is a rapid patternless manufacturing technology for sand molds based on the principle of droplet ejection [2]. For example, ExOne [3,4] and Voxeljet [5] utilize high-resolution combined array nozzles for spraying low-viscosity adhesives to achieve rapid manufacturing of casting sand molds.

The forming process of sand mold 3D printing technology is composed of a coating process, a printing process, and post-processing. In each forming process, the influences of the forming device and process parameters affect forming quality. The state of sand particles affects the flowability and accumulation of sand particles, significantly impacting the quality of sand layers [6]. The thickness of a sand layer is related to the accuracy of a 3D-printed sand mold. When a sand layer is thicker, the stepping effect of a 3D-printed sand mold is more significant. When a sand layer is thinner, the influences of the sand particle state and coating process parameters on its quality are more significant. In general, the thickness of a sand layer should be three times the diameter of sand particles [7]. Parteli and Pöschel [8] analyzed the processes of pushing and extruding powder particles during the movement of a spreading roller. The uniformity and smoothness of the surface of a powder layer during the

coating process were analyzed. A functional curve that relates surface roughness to the movement speed of the spreading roller was established. The bulk density of the sand layer directly affects the density of the final sand mold, which considerably influences the mechanical and casting properties of the mold [9]. The amount of adhesive used significantly affects the strength and precision of a printed sand mold. When the adhesive dose is higher, the strength of the sand mold is greater. The accuracy of a printed sand mold initially increases and then decreases with an increase in adhesive dose [10]. This phenomenon is related to the penetration of the adhesive into the sand layers [11]. The scanning printing mode of the 3D printing processes and the layered manufacturing concept make sand molds anisotropic. Research has shown that the bending strength of a sand mold along the scanning direction is approximately 10% higher than that perpendicular to the scanning direction [12]. In addition, the strength of a sand mold along the layer thickness direction is relatively low. Ma et al. [13] systematically studied penetration error analysis and compensation technology in sand mold 3D printing processes and proposed a penetration error compensation method based on a standard triangle language model. Current sand mold 3D printing technology requires post-processing, which primarily aims to accelerate the curing speed of adhesives and increase the strength of sand molds. Post-processing methods include visible light exposure, heating, and pressurization [14]. Nyembwe et al. [15] conducted a comparative test between post-processed and untreated sand molds. Post-processing temperature was 110 °C and heating time was 2 h. They found that post-processing can effectively improve the mechanical properties (e.g., tensile strength, bending strength, and surface hardness) of sand molds. When the adhesive content of a sand mold is higher, the improvement of its mechanical properties due to post-processing is more significant. However, post-processing slightly reduces the surface quality of sand molds. Mitra et al. [16] studied the effects of different post-processing temperatures and heating times on the mechanical properties, ablation, and gas permeability of printed sand molds. Various studies have shown that excessive post-processing temperatures significantly reduce the mechanical strength of sand molds. When heating temperature is approximately 100 °C and heating time is within the range of 0–5 h, the mechanical properties of printed sand molds improve. However, the ablation amount of a sand mold increases continuously as heating time increases. Sand mold 3D printing technology exhibits strong flexibility in manufacturing. Hawaldar and Zhang [17] compared the traditional sand manufacturing and sand mold 3D printing manufacturing processes. Sand mold 3D printing technology demonstrates evident advantages in production efficiency, material saving, and casting cleaning. Sama et al. [18] changed the simple design of traditional runners and adopted a complex runner design with better filling effect

to make the filling of liquid metal smooth and effectively prevent casting defects. Deng et al. [19–21] of Tsinghua University used sand mold 3D printing technology to achieve considerable systematic research in the manufacture of sand patterns with hollow structures.

At present, sand mold 3D printing technology and equipment exhibit the following limitations: Only single-material sand molds can be manufactured and manufactured sand molds require post-processing. The current study proposes a novel digital high-efficiency print forming method and device for multi-material sand molds. The proposed method enhances the flexible manufacturing capability of sand mold 3D printing technology, realizes high-efficiency manufacturing of casting sand molds, and broadens the application range of sand mold 3D printing technology.

2 High-efficiency print forming method and device for multi-material sand molds

The proposed high-efficiency print forming method for multi-material sand mold includes multi-material sand mold printing, two-way coating and printing integration, and layered heating and compaction integration. The specific processes included in the proposed method are described as follows.

2.1 Print forming method for multi-material sand molds

A multi-material sand mold includes two or more sand particle materials, allowing the sand mold to exhibit various properties based on the characteristics of various materials. A multi-material sand mold can be formed in accordance with these characteristics by combining a number of single-material sand molds, as shown in Fig. 1(a), or different types of multi-material sand molds that are formed on the basis of different sand particle ratios, as shown in Fig. 1(b).

The proposed multi-material sand mold 3D print forming method is appropriate for manufacturing sand molds with two or more sand particle materials. This method primarily includes the deposition of multi-material sand layers and the bonding of a multi-material sand mold, as shown in Fig. 2. Each sand layer is first divided into a checkerboard grid structure, where grid size represents the size of the smallest unit of each material for the sand mold, as shown in Fig. 2(a). The white, gray, yellow, and green grids represent the sand particles of four different materials. After a multi-material sand layer is deposited, a resin adhesive is sprayed onto the surface of the checkerboard multi-material sand layer following model information and realizing the printing of a multi-material sand mold, as shown in Fig. 2(b). The red hatched area represents the printed multi-material sand mold. The inner and outer contour surfaces of the printed sand mold adopt

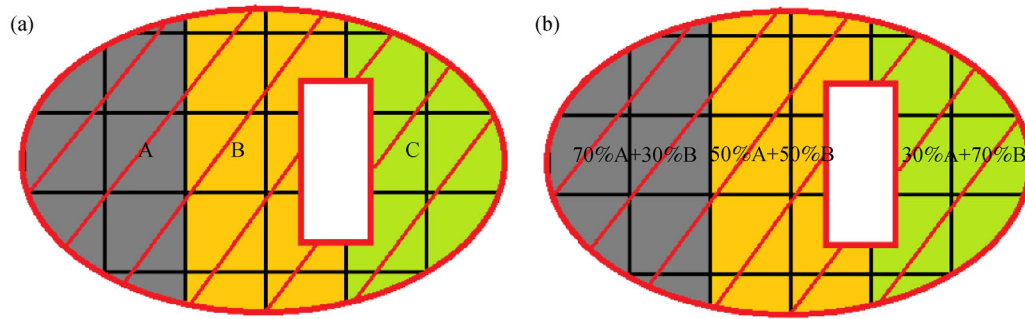


Fig. 1 Schematics of multi-material sand molds: (a) Combination of a number of single-material sand molds and (b) combination of different types of multi-material sand molds.

fine sand grains that can ensure that the sand mold has high contour precision, as shown in the gray grids of Fig. 2(b). However, the process also causes the sand mold to have poor air permeability. To address this issue, coarse sand grains are used inside the sand mold to improve permeability, as shown in the green grids of Fig. 2(b). Moreover, sand grains with good thermal conductivity can be used at the hot section of casting to improve the influence of the thermal joint, as shown in the yellow grids of Fig. 2(b).

2.2 Integrated forming method for two-way coating and printing

The proposed two-way coating and printing integrated 3D print forming method (Fig. 3) adopts a two-way coating and printing integrated device. In particular, the printing device is fixed between two sets of coating devices with opposite coating directions, as shown in Fig. 3(c). In the beginning of the coating process, coating device 1 on the left side of the print head moves at a certain coating speed. At this time, the print head begins to print an adhesive along the X axis after entering the forming box while coating device 2 on the right side of the print head does not operate, as shown in Fig. 3(a). When the sand mold for the current layer is completed, the two-way coating and

printing integrated device moves from one side of the forming box to the other side. At this time, the working platform moves down by a certain layer thickness and coating device 2 begins to deposit a sand layer. The print head begins printing negative along the X axis after entering the forming box while coating device 1 does not operate, as shown in Fig. 3(b). A sand mold is manufactured by repeating this process. This method efficiently combines the coating and printing processes, removes idle strokes from these processes, and shortens the overall 3D printing process for sand molds.

2.3 Integrated forming method for layered heating and compaction

To improve the strength of printed sand molds and reduce or eliminate the influence of post-processing on the deformation of printed sand molds, this study proposes a novel integrated forming method for layered heating and compaction to achieve superior control of the performance and precision of printed sand molds. The compacting and layered heating devices are illustrated in Fig. 4. The compacting device is installed on the opposite side of the cylindrical mounting bracket relative to the hopper. During the coating process, the roller moves horizontally and does not rotate. As sand particles continuously enter the

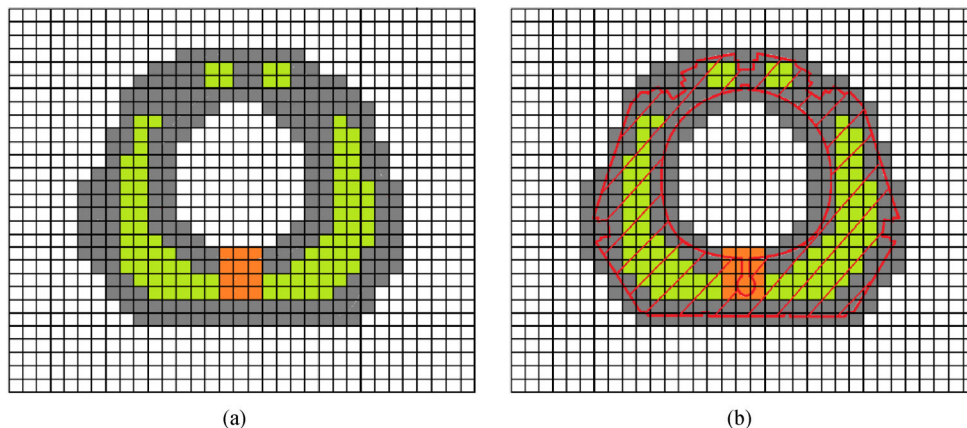


Fig. 2 Multi-material sand mold 3D print forming method: (a) Multi-material sand layer and (b) mold.

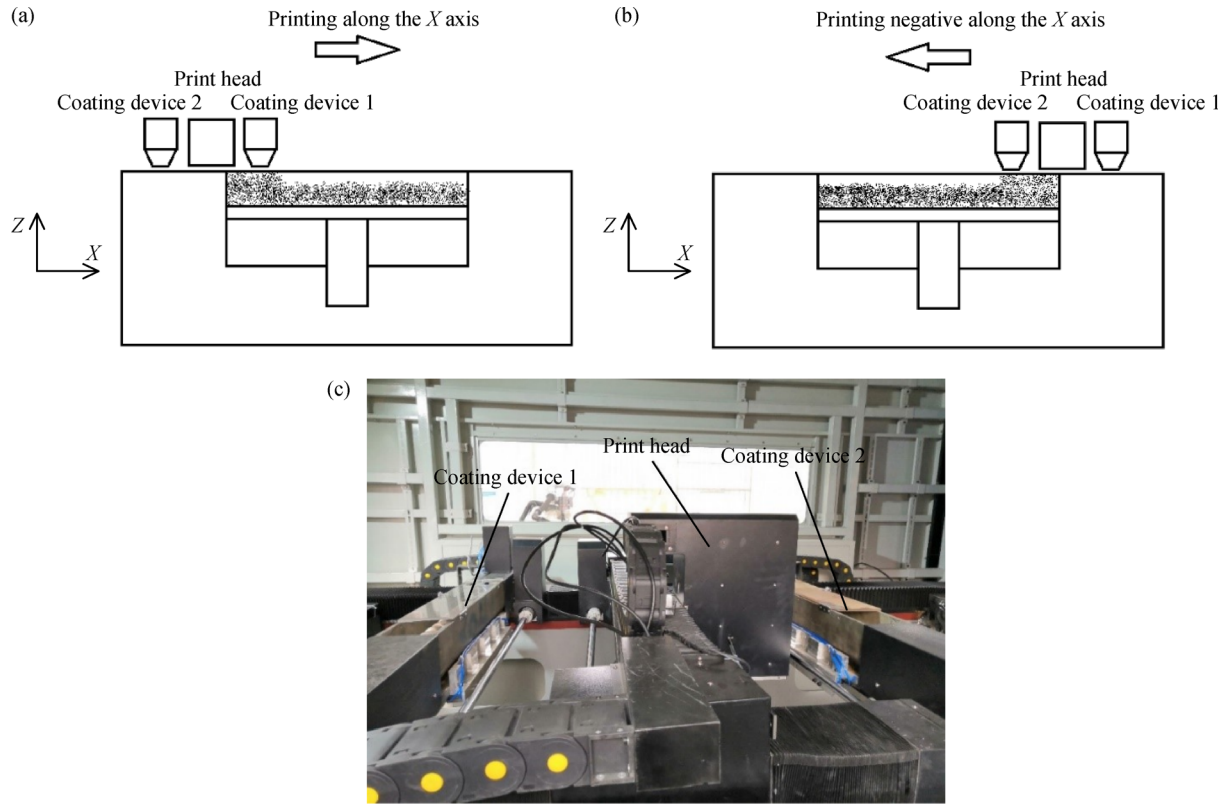


Fig. 3 Two-way coating and printing integration forming method: (a) Forward printing process; (b) reverse printing process; and (c) photograph of two-way coating and printing integration device.

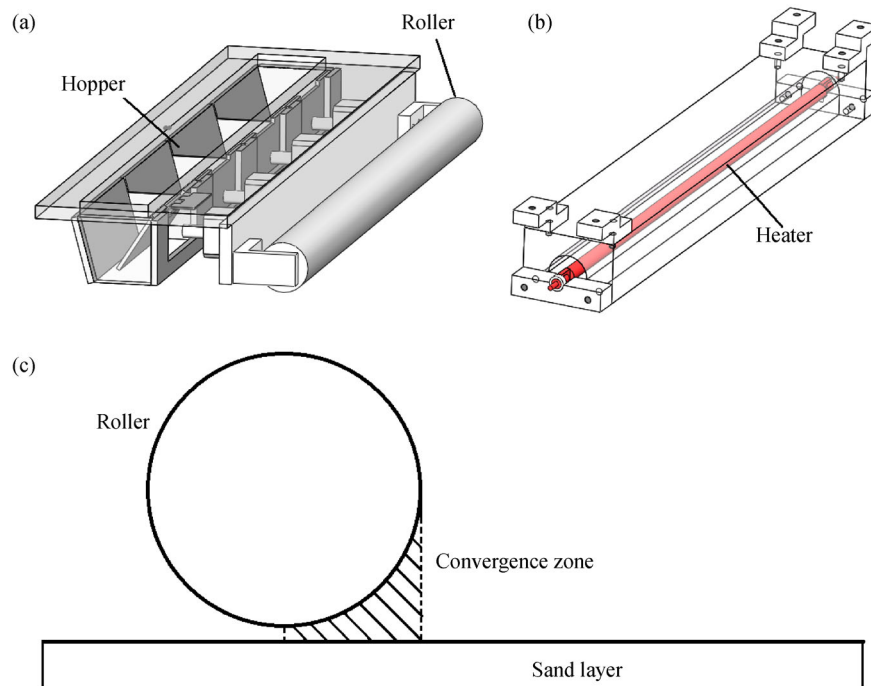


Fig. 4 Layered heating and compaction devices: (a) Coating and compaction device; (b) heating device; and (c) compaction schematic.

convergence zone formed by the surface of the circular roller, the contact angle between the roller and the surface of the sand layer is typically zero. Therefore, the sand layers are subjected to large compressive forces during the coating process, resulting in dense sand layers. The layered heating device is composed of a heating tube and a mounting frame. An infrared carbon fiber heating tube has high electrothermal conversion efficiency. The printed sand mold is heated layer-by-layer as the heating device moves.

3 Efficient print forming processes

3.1 Integrated forming process for two-way coating and printing

The two-way coating and printing integrated 3D print forming process can be divided into continuous and intermittent forming processes, as shown in Fig. 5. In the former, the print nozzle uses a full-face design; that is, the effective printing width L_p of the print head is equal to the width D of the forming box. Therefore, the print head can print the current sand layer by moving only once. In the latter, the effective print width of the print head is smaller than the width of the forming box. The print head must reciprocate n times to complete the printing of the current sand layer. In addition, the scanning direction of the print head must be perpendicular to the movement direction of the print head. The two-way coating and printing integrated process is selected on the basis of user's requirements for equipment manufacturing efficiency and the cost of equipment manufacturing and maintenance.

The integrated forming efficiency of two-way coating and printing is defined by Eq. (1). This equation states that the manufacturing time T_{layer} of a single-layer sand mold is equal to the working time T_{printing} of the print head.

$$T_{\text{layer}} = T_{\text{printing}}. \quad (1)$$

The efficiency of conventional sand mold print forming

is defined by Eq. (2), where $T_{\text{non-printing}}$ is the time required for the print head to return to the initial position, T_{coating} is the time required for the coating process, and $T_{\text{non-coating}}$ is the time required for the coating device to return to the initial position.

$$T_{\text{layer}} = T_{\text{printing}} + T_{\text{non-printing}} + T_{\text{coating}} + T_{\text{non-coating}}. \quad (2)$$

Assuming that η_1 and η_2 are the speedup coefficients for the returns of the print head and coating device, respectively. Then, Eq. (2) can be expanded as follows:

$$T_{\text{layer}} = T_{\text{printing}}(1 + \eta_1) + T_{\text{coating}}(1 + \eta_2). \quad (3)$$

For the continuous forming process, $T_{\text{coating}} > T_{\text{printing}}$. When $T_{\text{coating}} = T_{\text{printing}}$ and $\eta_1 = \eta_2 = 0.5$, the fabrication efficiency of a sand mold can be increased by at least 200%. For the intermittent forming process, $T_{\text{coating}} < T_{\text{printing}}$. When $T_{\text{coating}} = T_{\text{printing}}$ and $\eta_1 = \eta_2 = 0.5$, the efficiency of fabricating a sand mold can be increased by up to 200%.

3.2 Integrated forming process for layered heating and compaction

In this study, the effects of different infrared heating voltage values on the strength of printed sand molds were analyzed experimentally for the integrated forming process of layered heating and compaction. Figure 6 illustrates the infrared heating process during sand mold 3D printing. The infrared heating tube is mounted under the Y beam of the print head in a manner that enables it to move and heat the surface of the sand layer. The temperature and movement speed of the infrared heating tube are the two major factors that affect the heat source input to the sand layer, as expressed by Eq. (4):

$$Q_{\text{sandmold}} = \delta_{\text{absorb}} V_{\text{scan}} Q_{\text{release}}(T_{\text{heater}}), \quad (4)$$

where Q_{sandmold} is the rate of heat absorption by the sand layer, δ_{absorb} is the heat absorption factor of the sand layer, V_{scan} is the movement speed of the infrared heating tube, and $Q_{\text{release}}(T_{\text{heater}})$ is the heat release rate of the infrared

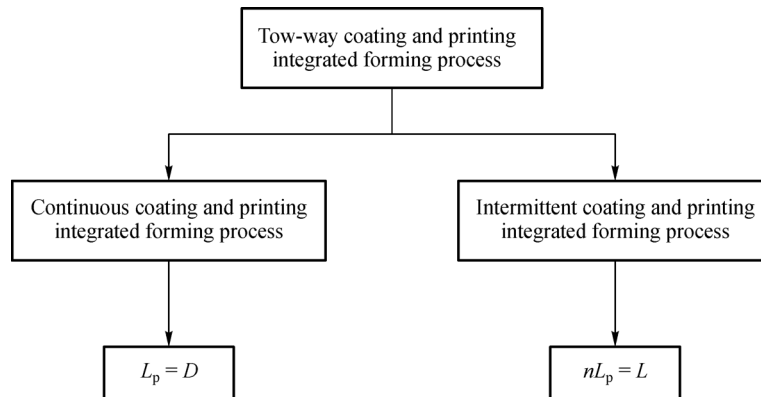


Fig. 5 Two-way coating and printing integrated forming process.

heating tube. $Q_{\text{release}}(T_{\text{heater}})$ is a function of the temperature of the heating tube. As the temperature of the heating tube increases, the amount of heat released also increases. Equation (4) indicates that the effects of V_{scan} and $Q_{\text{release}}(T_{\text{heater}})$ on Q_{sandmold} are the same. In the present study, the movement speed V_{scan} of the infrared heating tube was fixed at 36 mm/s and the heating tube temperature T_{heater} was considered a variable parameter for studying the performance of printed sand molds.

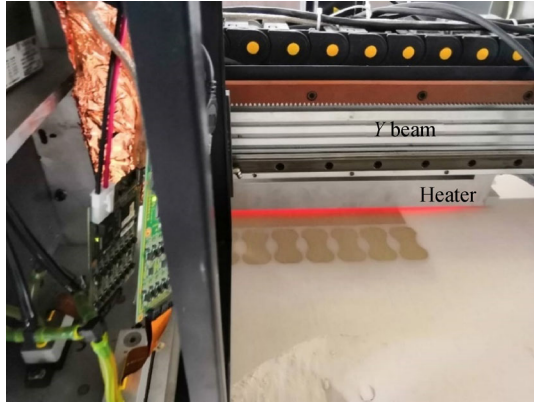


Fig. 6 Infrared heating process during sand mold printing.

In this study, the tensile strengths of printed sand molds with average infrared heating tube temperatures of 275 °C, 348 °C, 374 °C, 496 °C, and 539 °C were studied and compared with sand mold strength at 25 °C, wherein the resin injection amount was 1.7% and the curing agent content was 0.3%. Figure 7(a) presents the effects of infrared heating tube temperature on the tensile strength of printed sand molds. When the temperature of the infrared heating tube is between 275 °C and 374 °C, the tensile strength of the resulting sand molds is greater than that of a sand mold treated at room temperature. However, sand mold strength is significantly reduced when the temperature of the infrared heating tube reaches 496 °C. Sand mold strength at 539 °C is nearly zero. Meanwhile, the strength of the sand mold produced at 275 °C using the layered heating and compaction integrated forming process is 63.8% higher than those of sand molds printed using the same resin and curing agent content in previous studies, as shown in Fig. 7(b). Therefore, the proposed process can reduce the amount of resin required by approximately 30% while meeting the requirements for sand casting strength.

Figure 8 presents a sectional view of the printed sand molds at different infrared heating temperatures. For heating temperatures of 496 °C and 539 °C, the printed sand molds exhibit clear delamination because the infrared heating temperature is too high; that is, the curing speed of each layer of deposited sand is excessively fast. Therefore, the connection activity between resin printed on one layer and resin printed on the next layer is reduced, decreasing

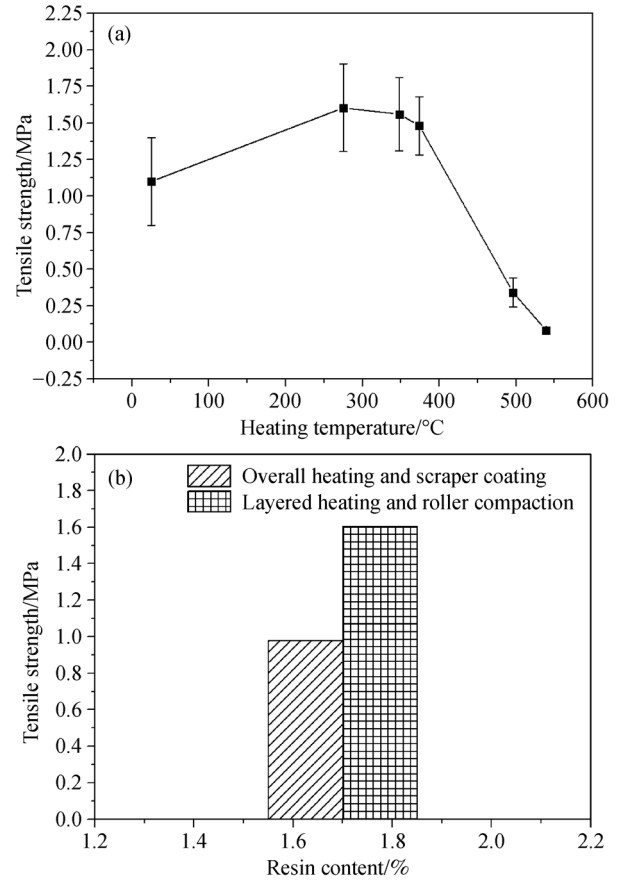


Fig. 7 Effects of infrared heating temperature on the tensile strength of printed sand molds: (a) Relationship between tensile strength and heating temperature and (b) comparison between the tensile strength of sand molds produced using two different processes.

the interlayer bonding ability of sand molds. When the infrared heating temperature is between 250 °C and 400 °C, the delamination of the 3D-printed sand molds is less evident. Hence, the temperature range can be selected as a preferred process parameter.

4 Case study

This study focused on the manufacture and casting of multi-material sand molds for typical pulley castings (Fig. 9). First, the bottom sand mold for a pulley was manufactured. This component is a multi-material 3D-printed sand mold deposited by a digital sand mold print forming machine. This mold is shown in Fig. 9(b), wherein the left part of the sand mold is the light green 3D-printed silica sand and its right part is the black 3D-printed chromite sand. The top sand mold for the pulley was machined with a patternless precision forming machine using silica sand, as shown in Fig. 9(a).

After the sand molds were manufactured, the top and

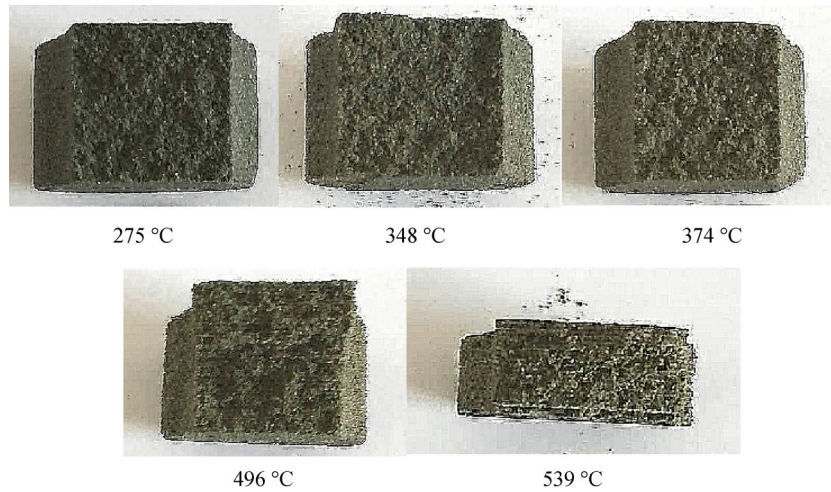


Fig. 8 Sections of printed sand molds at different infrared heating temperatures.

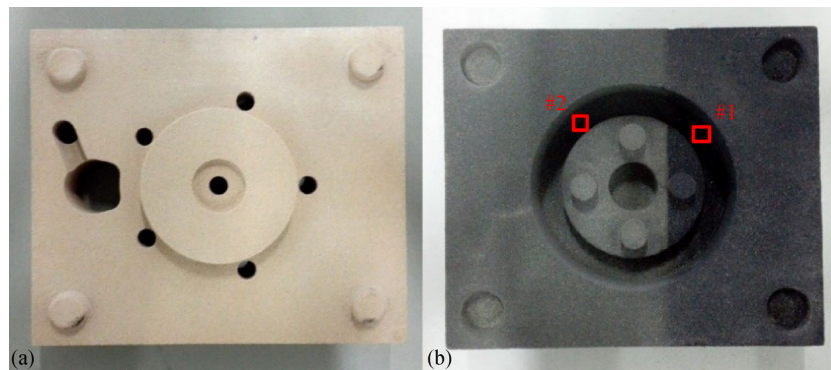


Fig. 9 Multi-material sand molds for the cast-iron parts of a typical pulley: (a) Top and (b) bottom sand molds.

bottom sand molds were combined and sealing paste was applied to the joint surface between the top and bottom sand molds. Subsequently, the pulley was cast, as shown in Fig. 10(a). After the molten metal cooled and solidified, a blank casting of the pulley was obtained, as shown in Fig. 10(b).

A microscopic metallographic examination of the cross section of the pulley blank was conducted in this study. Sample #1 is the graphite form of the surface layer and the core of the casting blank that corresponds to the silica sand mold. Sample #2 is the graphite form of the surface layer and the core of the casting blank that corresponds to the

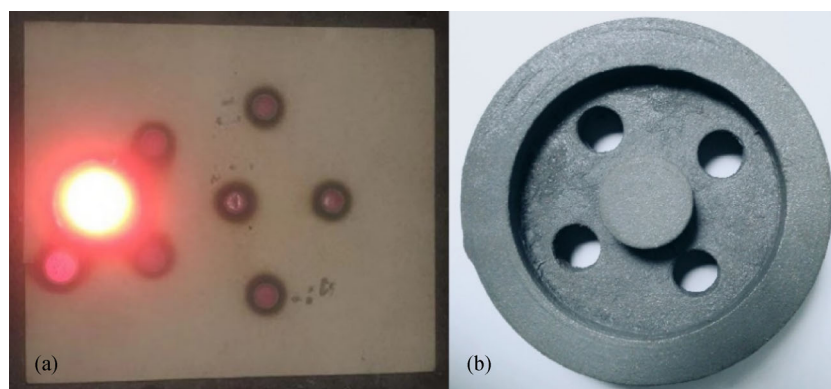


Fig. 10 Pouring of pulley castings: (a) Casting process and (b) casted blank.

chromite sand mold, as shown in Fig. 11. The surface graphite form of Sample #1 exhibits a mixed distribution of flaky directional E-type graphite and sheetlike A-type graphite. The core graphite form is a mixture of flaky A-type graphite and chrysanthemum-shaped B-type graphite. A small number of coarse graphite blocks and slight microscopic shrinkage also occur locally in this sample. The surface graphite form of Sample #2 is a mixed distribution of flaky directional E-type graphite and flaky A-type graphite. The core graphite form is flaky A-type graphite. A small number of graphite blocks and slight microscopic shrinkage also appear in Sample #2.

Graphite length was calculated by observing the graphite morphologies of Samples #1 and #2. The results are listed in Table 1. The average graphite length on the surface of Sample #2 is relatively small because the chromite sand mold exhibits high thermal conductivity, leading to a quenching effect during casting solidification and providing the casting with a fine-grained surface

structure. However, this phenomenon exerts a weaker effect on core graphite.

In addition, the tensile strength of the cast blanks was tested. The results are listed in Table 2. The pulley blank has a thick rim, and thus, shrinkage porosity is easy to produce at the hot joint where the rim and spoke intersect during the solidification of casting, resulting in significantly lower tensile strength at the hot section of casting. A comparison of the tensile test results of Samples #1 and #2 shows that the chromite sand mold exerts a positive effect on the strength of the hot section of casting, increasing tensile strength by 22.5%.

5 Conclusions

To address the problems of high sand resin consumption, low manufacturing efficiency, and poor flexibility in the manufacturing ability of sand mold 3D printing

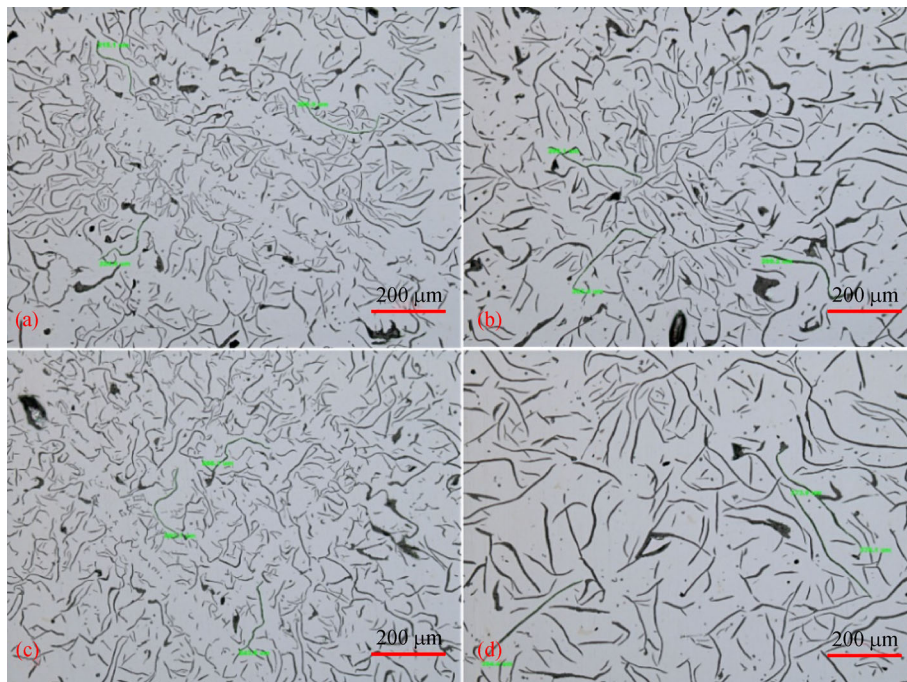


Fig. 11 Cross-sectional graphite formed at the intersection of the pulley blank's rim and spoke: (a) #1 surface layer, (b) #1 core, (c) #2 surface layer, and (d) #2 core.

Table 1 Cross-sectional graphite length at the intersection of the pulley blank's rim and spoke

| Sample | Graphite length/ μm | | | | Level |
|------------|--------------------------------|-----------------|-----------------|---------------|-------|
| | Field of view 1 | Field of view 2 | Field of view 3 | Average value | |
| #1 surface | 243 | 268 | 277 | 263 | 3 |
| #1 core | 294 | 338 | 465 | 367 | 3 |
| #2 surface | 227 | 229 | 247 | 234 | 4 |
| #2 core | 287 | 337 | 437 | 354 | 3 |

Table 2 Cross-sectional tensile strength at the intersection of the pulley blank's rim and spoke

| Sample | Tensile strength/MPa | | | Average tensile strength/MPa |
|--------|----------------------|--------|--------|------------------------------|
| | Test 1 | Test 2 | Test 3 | |
| #1 | 124 | 142 | 136 | 133 |
| #2 | 148 | 161 | 179 | 163 |

technology, a multi-material sand mold digital high-efficiency print forming method and device were proposed in this study.

1) A multi-material sand mold high-efficiency printing and forming method was proposed. The method was based on a multi-material sand mold print forming, two-way coating and printing integrated forming, and layered heating and compaction integrated forming methods. The proposed approach can realize high-performance multi-material composite sand molds and highly efficient manufacturing.

2) We proposed a two-way coating and printing integrated forming process that can increase the efficiency of sand mold manufacturing by 200% compared with typical sand mold 3D printing technology. The tensile strength of sand molds produced using the integrated forming process of layered heating and compaction increased by 63.8% compared with the tensile strength of sand molds produced via typical 3D printing technology. That is, the resin amount required for a sand mold can be reduced by approximately 30%.

3) The manufacture and casting of a multi-material sand mold of a typical pulley casting were conducted. The surface graphite length of the casting that corresponded to the chromite sand mold was smaller than that of the casting that corresponded to the silica sand mold. Furthermore, the chromite sand mold exerted a positive effect on the tensile strength of the hot section of casting, increasing tensile strength by 22.5%.

Acknowledgements This research was supported by the National Excellent Young Scientists Fund (Grant No. 51525503).

References

- Shan Z, Qin S, Liu Q, et al. Key manufacturing technology & equipment for energy saving and emissions reduction in mechanical equipment industry. *International Journal of Precision Engineering and Manufacturing*, 2012, 13(7): 1095–1100
- Yan Y, Li S, Zhang R, et al. Rapid prototyping and manufacturing technology: Principle, representative technics, applications, and development trends. *Tsinghua Science and Technology*, 2009, 14 (Suppl 1): 1–12
- Hackney P M, Wooldridge R. Characterisation of direct 3D sand printing process for the production of sand cast mould tools. *Rapid Prototyping Journal*, 2017, 23(1): 7–15
- Mostafaei A, Stevens E L, Ference J J, et al. Binder jetting of a complex-shaped metal partial denture framework. *Additive Manufacturing*, 2018, 21: 63–68
- Budzick G, Markowski T, Kozik B, et al. The application of Voxeljet technology to the rapid prototyping gear cast. *Archives of Foundry Engineering*, 2014, 14(1): 87–90
- Shan Z, Guo Z, Du D, et al. Coating process of multi-material composite sand mould 3D printing. *China Foundry*, 2017, 14(6): 498–505
- Sachs E M, Cima M J, Caradonna M A, et al. Jetting layers of powder and the formation of fine powder beds thereby. US Patent, 6596224. 2003-07-22
- Parteli E J R, Pöschel T. Particle-based simulation of powder application in additive manufacturing. *Powder Technology*, 2016, 288: 96–102
- Hu C, Du W. Research on the method for improving mechanical properties of sand mould based on 3D printing process. *Materials Science and Engineering*, 2018, 394: 1–6
- Xue L, Hu C, Li X, et al. Research on the influence of furan resin addition on the performance and accuracy of 3D printing sand mould. *Materials Science and Engineering*, 2018, 392: 1–6
- Yang W, Jia P, Ma Y, et al. Modeling and simulation of binder droplet infiltration in 3D printing technology. *Nanotechnology and Precision Engineering*, 2017, 15(4): 246–253 (in Chinese)
- Thiel J, Ravi S, Bryant N. Advancements in materials for three-dimensional printing of molds and cores. *International Journal of Metalcasting*, 2017, 11(1): 3–13
- Ma X, Lin F, Zhang L. The heterogeneous compensation for the infiltrative error of binder jetting additive manufacturing process. In: *Proceedings of the 26th International Solid Freeform Fabrication Symposium*. Austin: The University of Texas at Austin, 2015
- Brodin D, Panzera C, Panzero P. Dental restorations formed by solid freeform fabrication methods. US Patent, 6994549. 2006-02-07
- Nyembwe K, Mashila M, van Tonder P J M, et al. Physical properties of sand parts produced using a Voxeljet VX1000 three-dimensional printer. *South African Journal of Industrial Engineering*, 2016, 27(3): 136–142
- Mitra S, Rodríguez de Castro A, El Mansori M. The effect of ageing process on three-point bending strength and permeability of 3D printed sand molds. *International Journal of Advanced Manufacturing Technology*, 2018, 97(1–4): 1241–1251
- Hawaldar N, Zhang J. A comparative study of fabrication of sand casting mold using additive manufacturing and conventional process. *International Journal of Advanced Manufacturing Technology*, 2018, 97(1–4): 1037–1045
- Sama S R, Wang J, Manogharan G. Non-conventional mold design for metal casting using 3D sand-printing. *Journal of Manufacturing*

- Processes, 2018, 34: 765–775
19. Deng C, Kang J, Shangguan H, et al. Effects of hollow structures in sand mold manufactured using 3D printing technology. *Journal of Materials Processing Technology*, 2018, 255: 516–523
 20. Shangguan H, Kang J, Deng C, et al. 3D-printed rib-enforced shell sand mold for aluminum castings. *International Journal of Advanced Manufacturing Technology*, 2018, 96(5–8): 2175–2182
 21. Deng C, Kang J, Shangguan H, et al. Insulation effect of air cavity in sand mold using 3D printing technology. *China Foundry*, 2018, 15(1): 37–43